DEVELOPMENT OF SCIENCE

ISNN 3030-3907

2026 AUGUST

ISSUE - 8
VOLUME -1

DEVELOPMENT OF SCIENCE

D E V O S

РАЗВИТИЕ НАУКИ

ILM-FAN TARAQQIYOTI

Development of science

Scientific journal
Ilmiy jurnal
Научный журнал

AUGUST 2026
Issue - 8, VOLUME - 1

ISSN 3030 -3907

*The scientific journal **«Development of Science»** was registered by the State on April 15, 2024 with certificate number №256445.*

***«Ilm fan tarqqiyoti»** ilmiy jurnali 2024 yil 15 aprel kuni №256445 sonli guvohnoma bilan Davlat ro'yxatidan o'tgan.*

*Научный журнал **«Развитие науки»** был зарегистрирован государством 15 апреля 2024 года под номером свидетельства № 256445.*

The proceedings will be provided to the authors in electronic form (PDF format). The authors bear full responsibility for the content of the articles included in the proceedings, the accuracy and reliability of the statistical data and regulatory documents cited therein, as well as for any opinions and judgments expressed in their articles. Articles that do not meet the established requirements will not be included in the proceedings. The Organizing Committee reserves the right to shorten the text of an article, make minor editorial corrections, and assign submissions to the appropriate sections.

To'plam elektron ko'rinishda (pdf formatida) mualliflarga taqdim etiladi. To'plamga kiritiladigan maqolalarning mazmuni, ulardagi statistik ma'lumotlar va me'yoriy hujjatlarning to'g'riligiga hamda har qanday fikr - mulohazalarga mualliflarning o'zlari mas'ul hisoblanadilar.Talablarga javob bermaydigan maqolalar to'plamga kiritilmaydi. Tashkiliy qo'mita maqola matnini qisqartirish, qisman tuzatish kiritish, seksiyalarga joylashtirish huquqiga ega.

Сборник предоставляется авторам в электронном виде (в формате PDF). Авторы несут полную ответственность за содержание статей, включённых в сборник, достоверность приведённых в них статистических данных и нормативных документов, а также за изложенные мнения и суждения. Статьи, не соответствующие установленным требованиям, в сборник не включаются. Организационный комитет оставляет за собой право сокращать текст статьи, вносить отдельные редакционные исправления и распределять материалы по соответствующим секциям.

EDITOR-IN-CHIEF:
Temirov Alisher Hashim oglu - Doctor of Philosophy (PhD) in Technical Sciences, Associate Professor.
CHAIRMAN OF THE EDITORIAL BOARD:
Fozilov Sadriddin Fayzullayevich - Doctor of Technical Sciences, Professor
MEMBERS OF THE EDITORIAL BOARD:

Faheem Uddin
Professor,Iqra university, Pakistan
Siddikova Sadokat Gafforovna
DSc, Rector of Bukhara State Technical University, Uzbekistan
Dr. Amit Rawal
Professor, Department of Textile and Fibre Engineering Indian Institute of Technology Delhi, India
Alexander Vitalievich Dudan
Associate Professor, Euphrosyne Polotskaya State University of Polotsk, Republic of Belarus
Bozorov Gayrat Rashidovich
Professor Bukhara State Technical University, Uzbekistan
Vladimir Mikhailovich Kapustin
Professor,Gubkin Russian State University of Oil and Gas (National Research University),Russian Federation
Shaoliang Chen
Ph. D., Engineer,Cement Science and New Building Materials Research Institute, China
Tukhtayeva Zebo Sharifovna
Bukhara State Technical University, Professor.
Kodirov Abduakhad Abdurakhimovich
Karshi State University, Professor
Turemuratov Sharibay Naurizbaevich
General Scientific Secretary of the Karakalpakstan Branch of the Academy of Sciences of the Republic of Uzbekistan, Professor
Tursunov Kakhor Shonazarovich
Karshi State University, Professor
Sharipov Muzaffar Samandarovich
Bukhara State University, Professor.
Alikulov Rustam Valiyevich
Termez State University, Professor
Makhmudov Mukhtar Jamolovich
Bukhara State Technical University, Professor.
Oral Kurganbekovich Beyseynbayev
Professor,M. Auezov South Kazakhstan University,Republic of Kazakhstan
Tropov Khamza Tursunovich
Samarkand State University, Professor
Nizamov Aslitdin Badreddinovich
Bukhara State Technical University, Professor.
Saidakhmedova Nodira Ilkhomovna
Tashkent State University of Economics, Professor

ORGANIZATIONAL STRUCTURE:

Safarov J.A.-*editor*
Panoyev N.Sh. -*editor*
Buranov N.G. -*assistant editor*
Shodiyev D.X.- *layout editor*
Izzatov D.X. - *layout editor*
Urinov J.B. - *layout editor*
Temirov A.T. - *graphic designer*
Temirov I.G. – *layout designer*

Changes to the composition of the Editorial Board, including the appointment of new members or the removal of existing members, shall be made by the Editor-in-Chief.

www.devos.uz

ISSN 3030-3907

BLACK POWDER IN NATURAL GAS TRANSMISSION SYSTEMS: EDXRF CHARACTERIZATION AND METROLOGICAL IMPLICATIONS

Ozoda Bakhranovna. Akhmedova
Tashkent State Technical University named after Islam Karimov University Street 2, Tashkent 100095, Uzbekistan
Email: zodamedova@gmail.com
Sh.M.Isamadinov
Chief Engineer, Fergana Main Gas Pipeline Administration, JSC Uztransgaz, Fergana, Uzbekistan
A.Sh.Qayumov
Tashkent State Technical University named after Islam Karimov University Street 2, Tashkent 100095, Uzbekistan
M.B.Akhmedova
Bukhara State Technical University K. Murtazayev Street 15, Bukhara 200117, Uzbekistan

Abstract. Mixed deposits comprising corrosion products, mineral particles, condensate, and heavy hydrocarbons can accumulate in filters and orifice-based metering units at gas distribution stations, thereby reducing the accuracy of natural gas flow measurement. This study aimed to determine the elemental composition of pipeline deposits locally referred to as perafor or black powder and to assess their potential influence on differential-pressure gas metering. A deposit sample collected from a gas transmission system was analysed using energy-dispersive X-ray fluorescence spectrometry. The elemental mass fractions were calculated using the fundamental parameters method, and the analysis was repeated three times to verify the reproducibility of the results. The estimated carbon content was 71.60 mass%, while the principal directly detected elements were Fe at 16.30 mass%, S at 6.58 mass%, Si at 1.30 mass%, Cl at 1.22 mass%, and Ca at 1.18 mass%. The results indicate that the deposit is a complex heterogeneous mixture of carbonaceous binders, iron-containing corrosion products, sulfur-containing compounds, and mineral particulates rather than solely soot or rust. Accumulation of this material on the orifice bore and upstream edge reduces the effective flow area, artificially increases the differential pressure, and may consequently result in overestimation of the measured gas flow rate. The findings demonstrate the importance of deposit monitoring and support the targeted application of dispersants upstream of filters and metering units, particularly in pipeline sections prone to moisture and condensate formation. The results can contribute to improving the operational reliability and measurement accuracy of natural gas transmission systems.

ISSN 3030-3907

Keywords: natural gas transmission pipeline; black powder; pipeline deposits; EDXRF; orifice flow measurement; differential pressure; corrosion products; gas metering; dispersant.

Annotatsiya. Korroziya mahsulotlari, mineral zarrachalar, kondensat va og'ir uglevodorodlarni o'z ichiga olgan aralash konlar gaz taqsimlash stansiyalaridagi filtrlar va teshikli o'lchash qurilmalarida to'planishi mumkin, bu esa tabiiy gaz oqimi o'lchovining aniqligini pasaytiradi. Ushbu tadqiqot mahalliy darajada perafor yoki qora kukun deb ataladigan quvur liniyasi konlarining elementar tarkibini aniqlash va ularning differentsial bosimli gazni o'lchashga potentsial ta'sirini baholashga qaratilgan. Gaz uzatish tizimidan olingan kon namunasi energiya-dispersiv rentgen floresans spektrometriyasi yordamida tahlil qilindi. Elementar massa fraksiyalari asosiy parametrlar usuli yordamida hisoblab chiqilgan va natijalarning takrorlanishi tekshirilishi uchun tahlil uch marta takrorlangan. Taxminiy uglerod tarkibi 71,60 massa % ni tashkil etdi, asosiy aniqlangan elementlar esa Fe 16,30 massa% da, S 6,58 massa% da, Si 1,30 massa% da, Cl 1,22 massa% da va Ca 1,18 massa%da. Natijalar shuni ko'rsatadiki, depozit faqat kuyikish yoki zang emas, balki uglerodli bog'lovchilar, temir o'z ichiga olgan korroziya mahsulotlari, oltingugurt o'z ichiga olgan birikmalar va mineral zarrachalarning murakkab heterojen aralashmasidir. Ushbu materialning teshik teshigi va yuqori oqim chetida to'planishi samarali oqim maydonini kamaytiradi, differentsial bosimni sun'iy ravishda oshiradi va natijada o'lchangan gaz oqim tezligini ortiqcha baholashga olib kelishi mumkin. Topilmalar depozit monitoringining muhimligini namoyish etadi va dispersantlarni filtrlar va o'lchash moslamalarining yuqori qismida, ayniqsa namlik va kondensat hosil bo'lishiga moyil bo'lgan quvur liniyalarida maqsadli qo'llanilishini qo'llab-quvvatlaydi. Natijalar tabiiy gaz uzatish tizimlarining ekspluatatsion ishonchliligi va o'lchov aniqligini oshirishga yordam beradi.

Kalit so'zlar: tabiiy gazni uzatish quvuri; qora kukun; quvur liniyasidagi konlar; EDXRF; teshik orqali oqimni o'lchash; differentsial bosim; korroziya mahsulotlari; gazni o'lchash; dispersant.

Аннотация. Смешанные отложения, содержащие продукты коррозии, минеральные частицы, конденсат и тяжелые углеводороды, могут накапливаться в фильтрах и дозирующих устройствах на газораспределительных станциях, тем самым снижая точность измерения расхода природного газа. Целью данного исследования было определить элементный состав отложений на трубопроводах, которые в местных условиях называют перафором или черным порошком, и оценить их потенциальное влияние на измерение перепада давления газа. Образец

ISSN 3030-3907

отложений, взятый из газотранспортной системы, был проанализирован с помощью энергодисперсионной рентгенофлуоресцентной спектрометрии. Массовые доли элементов были рассчитаны с использованием метода фундаментальных параметров, и анализ был повторен три раза для проверки воспроизводимости результатов. Предполагаемое содержание углерода составило 71,60 мас.%, в то время как основными непосредственно обнаруженными элементами были Fe - 16,30 мас.%, S - 6,58 мас.%, Si - 1,30 мас.%, Cl - 1,22 мас.% и Ca - 1,18 мас.%. Результаты показывают, что отложения представляют собой сложную гетерогенную смесь углеродистых связующих, железосодержащих продуктов коррозии, серосодержащих соединений и минеральных частиц, а не только сажу или ржавчину. Скопление этого материала на отверстии и входной кромке уменьшает эффективную площадь потока, искусственно увеличивает перепад давления и, следовательно, может привести к завышению измеренного расхода газа. Полученные результаты демонстрируют важность мониторинга отложений и способствуют целенаправленному применению диспергаторов перед фильтрами и дозирующими узлами, особенно на участках трубопроводов, подверженных образованию влаги и конденсата. Результаты могут способствовать повышению эксплуатационной надежности и точности измерений в системах транспортировки природного газа.

Ключевые слова: газопровод для транспортировки природного газа; сажа; отложения на трубопроводе; EDXRF; измерение расхода через диафрагму; перепад давления; продукты коррозии; дозирование газа; диспергатор.

INTRODUCTION.

Main natural-gas transmission pipelines are used in the Republic of Uzbekistan to transport natural gas and deliver it to socially important consumers, including households and public-sector institutions, as well as wholesale consumers, compressed-natural-gas filling stations, and strategically important facilities such as thermal power plants and mineral-fertilizer production enterprises. Main gas pipelines receive natural gas from compressor stations and deliver it to consumers through gas distribution stations (GDSs). A gas distribution station is a technological facility designed to receive natural gas from a main pipeline, reduce its pressure, meter and purify the gas, and distribute it to consumers [1].

Depending on their service coverage, gas distribution stations are divided into two types:

ISSN 3030-3907

1. Main GDSs, which primarily serve cities with large numbers of consumers or major industrial facilities.

2. Local GDSs, which serve districts, villages, or small production enterprises with comparatively fewer consumers.

The main functional units of a gas distribution station are as follows:

1. Inlet unit, which receives natural gas from the main gas pipeline.
2. Filters, which retain, as far as practicable, “perafor” and other foreign materials contained in the natural gas.
3. Pressure regulators, which stabilize the natural-gas pressure at the specified level.
4. Metering unit, which determines the natural-gas flow rate.
5. Safety valves, which monitor excessive pressure and protect the system against overpressure.
6. Odorant storage vessel, which stores ethyl mercaptan used for natural-gas odorization.
7. Outlet headers, which distribute the natural gas to consumer networks.

At present, the year-by-year decline in available natural-gas resources and the need to deliver gas safely to residential, wholesale, and compressed-natural-gas filling-station consumers make accurate accounting of every cubic metre of supplied gas an increasingly important task. Under these conditions, it is appropriate to install an electronic gas flow computer that complies with the applicable GOST requirements within the GDS metering complex [2–3].

The electronic gas flow computers currently installed at GDSs in Uzbekistan include AutoPilot, AutoPilot PRO, and Floobus units. These devices determine the flow rate of high-pressure natural gas passing through the metering assembly from the measured differential pressure. They are measurement-and-information systems that determine the natural-gas flow rate in real time, convert the measured values to standard conditions, and transmit the results to dispatching systems by telemetry; the stated accuracy class is ±1.5 %. The flow computer calculates the natural-gas flow rate from the pressure differential ΔP generated by a restriction device, namely an orifice plate, installed in the pipeline. A restriction device is a hydraulic element that reduces the flow cross-section inside the pipe, thereby changing the velocity and pressure of the stream and enabling the flow rate to be calculated from ΔP.

The operating principle of the restriction device is as follows: high-pressure natural gas passes through the orifice plate, the flow velocity increases, the static pressure decreases, and a differential pressure ΔP is generated between the upstream and downstream pressure-tapping points. The gas flow rate is then calculated from this differential pressure.

ISSN 3030-3907

The pressure signal generated in the sealed section containing the orifice plate is transmitted to the electronic flow computer through impulse lines.

Impulse lines are elements that establish a hydraulic connection between the natural-gas pipeline and the measuring instrument, such as a pressure or differential-pressure transmitter, and transmit the process-medium parameters without distortion. Two impulse lines are used: one for the positive-pressure side and one for the negative-pressure side.

During natural-gas transmission, contaminants and deposits accumulate on the orifice bore and on its upstream and downstream edges. In operating practice, this material is locally referred to as “perafor”. Perafor mainly consists of sand, dust, corrosion products, metal particles, and heavy hydrocarbons mixed with condensate.



Figure 1. Perafor contamination and deposits accumulated on the orifice plate and inside the adjacent pipeline section.

Several practical assumptions may be proposed regarding the formation of perafor:

1. Insufficient purification of the natural gas.
2. The presence of corrosion in the natural-gas pipeline.
3. The presence of moisture in the natural gas.
4. Inefficient operation of the natural-gas filters or failure to clean them at the required intervals.

This condition may adversely affect natural-gas accounting because the effective diameter of the orifice bore decreases, the differential pressure ΔP may be artificially increased, and the electronic flow computer may overestimate the gas flow rate. The deposits may also contribute to malfunction of process equipment, including ball valves, various control and safety valves, and pressure regulators operating within the GDS, and may reduce the thermal or operational efficiency of gas-consuming equipment installed at consumer facilities.

ISSN 3030-3907

Such operational problems not only threaten the reliable performance of the measuring instruments, but also interrupt gas delivery because the flow inside the pipeline must be stopped while the orifice plate is cleaned, and pressure control in the isolated line becomes more difficult. According to field observations, approximately 30–60 min is required to clean a contaminated orifice plate and return the metering line to service. During this period, gas-delivery interruption and a reduction in pressure in the isolated line may occur.

Factors contributing to perafor formation include localized pitting corrosion and under-deposit corrosion in pipelines. Moisture, internal corrosion, and ineffective filtration may be emphasized as the principal causes. Under these conditions, the key conclusion is that the problem is not pure “gas corrosion”, but a combination of moisture, condensate, solid particles, low-point deposits, and low-point corrosion. In gas-transmission pipelines, properly dried gas alone generally does not cause severe internal corrosion. Corrosion develops mainly when water condenses and forms an electrolyte with CO_2 or other aggressive components. Materials prepared for the Gas Research Institute/Internal Corrosion Direct Assessment (GRI/ICDA) approach for gas-transmission systems likewise indicate that internal corrosion commonly develops following an upstream gas-treatment upset that permits free water or another corrosive liquid to enter the pipeline. Guidance from the Pipeline and Hazardous Materials Safety Administration (PHMSA) also indicates that sales-quality dry gas does not normally corrode the internal surface and that the problem begins when water condenses. Thermodynamic hydrate inhibitors such as methanol or monoethylene glycol can help prevent hydrate formation by reducing moisture; however, they do not eliminate sand, rust, metal particles, or heavy-hydrocarbon deposits and, in some cases, may become an additional factor affecting formation of an aqueous phase at pipeline low points.

The concentration of hydrogen sulfide in the transported gas is very low, at the ppm level. However, because carbon dioxide is present, corrosion of the metal may occur through the action of CO_2 in the presence of moisture. The principal simplified reactions are:

$$CO_2 + H_2O \rightarrow H_2CO_3 \text{ (carbonic acid)}$$

$$H_2CO_3 + Fe \rightarrow FeCO_3 + H_2$$

When the carbon-dioxide content of the transported gas exceeds approximately 0.5 %, the tendency toward corrosion may increase. Carbon-dioxide solubility increases particularly at elevated pressure, while corrosion can become active at moderate and low temperatures. Localized pitting corrosion may develop in the pipeline, accompanied by an increase in iron-carbonate ($FeCO_3$) deposits [4].

MATERIALS AND METHODS.

ISSN 3030-3907

To identify possible solutions to the operational problems described above, the component composition and physicochemical properties of the gas transported through the main gas pipeline were first examined (Tables 1 and 2).

Table 1.

Component composition of the natural gas sampled at the Khojaabad gas distribution station

No.	Component	mol %
1	CO_2	1.35
2	N_2	0.68
3	O_2	0.00
4	Methane (CH_4)	94.01
5	Ethane (C_2H_6)	3.28
6	Propane (C_3H_8)	0.52
7	i-Butane	0.06
8	n-Butane	0.06
9	i-Pentane	0.02
10	n-Pentane	0.02
11	Hexane	0.00

Table 2.

Properties of the natural gas sampled at the Khojaabad gas distribution station

No.	Facility	Gas density (kg/m^3)	Calorific value ($kcal/m^3$)	CO_2 (%)	N_2 (%)
1	Khojaabad GDS	0.716	8123	1.35	0.68
2	Gazli Main Gas Pipeline Administration	0.717	8009	0.977	1.866

Analysis of the natural gas sampled at the Khojaabad gas distribution station showed that the gas consisted predominantly of methane (94.01 mol %), while the CO_2 content was 1.35 mol %. Under high-pressure conditions (3–8 MPa) and in the possible presence of moisture, this level is considered sufficient to activate corrosion processes [5].

The practical problem is not pipeline corrosion alone, but accumulation in filters and at the orifice bore of perafor consisting of sand, dust, rust, corrosion products such as $FeCO_3$, metal particles, condensate, and heavy hydrocarbons. This deposit reduces the effective orifice diameter, may artificially increase ΔP, and can

ISSN 3030-3907

create a risk of overestimation of the gas flow rate. This represents one of the most significant adverse effects in the system.

Many GDS metering systems use electronic flow computers connected to differential-pressure transmitters and an orifice plate. For a geometrically compliant and hydraulically developed installation, the mass-flow rate is related to the pressure drop according to the standard orifice-meter relation:

$$q_m = (C\,\varepsilon / \sqrt{(1 - \beta^4)})\,(\pi d^2/4)\,\sqrt{(2\Delta p\,\rho_1)} \quad (1)$$

where q_m is the mass-flow rate, C is the discharge coefficient, ε is the expansibility factor, $\beta = d/D$ is the diameter ratio, d is the orifice bore, D is the pipe internal diameter, Δp is the differential pressure, and ρ_1 is the upstream density. Deposits that modify the bore, upstream edge, surface roughness, pressure-tap condition, or local flow profile can therefore change the measurement response

To identify an appropriate solution for protecting the electronic gas flow computer against the principal adverse influence in the system, the composition of the contaminants and deposits accumulated on the orifice bore and on the upstream and downstream edges during natural-gas transmission was determined.

The black powder (perafor) sample was collected from the orifice-metering assembly of a gas distribution station and transported to the laboratory in a hermetically sealed container. A representative laboratory portion was separated, dried at 40 ± 5 °C to constant mass, and cooled in a desiccator. The dried sample was deagglomerated, reduced to a particle-size fraction of <75 μm, and homogenized. For EDXRF analysis, 4.0 ± 0.1 g of the sample was placed in a 32/40 mm XRF sample cup fitted with a 4 μm Prolene film. Three independent test portions were prepared. The instrument was operated in the NEX CG II configuration over the Na–U elemental range, using selected secondary-target channels and validated counting times. Quantitative analysis was performed using the fundamental-parameters method and matrix-matched reference materials. For calibration verification, an independent certified reference material, a blank, and a laboratory duplicate were measured in each analytical batch. The results were expressed as mean ± standard deviation (n = 3), together with the relative standard deviation, lower limit of detection, and lower limit of quantification. The C* value generated by the fundamental-parameters calculation was treated as a model-dependent balance estimate, while the oxide-equivalent values were regarded as software-normalized representations rather than direct identification of crystalline phases.

The perafor sample was analysed by energy-dispersive X-ray fluorescence spectrometry (EDXRF). The instrument employed 90° Cartesian geometry, indirect excitation through secondary targets, a 50 kV/50 W X-ray tube with a palladium anode, and a large-area silicon-drift detector (SDD); it was capable of

ISSN 3030-3907

direct detection of elements from Na to U [15]. The laboratory spectrum contained the Si, RX9, Cu, Mo, and Al secondary-target/polarizer channels. When the sample is excited by X-rays, characteristic fluorescence lines specific to each element are generated. The energy of each line is used to identify the element, while its intensity is used to calculate the mass fraction.

Quantification was performed by the instrument software using the fundamental-parameters (FP) method. The FP algorithm deconvolutes spectral lines, accounts for matrix absorption and enhancement effects, and normalizes the result in mass %. In the NEX CG II system, low-atomic-number constituents from hydrogen to fluorine, including carbon, may be estimated from scattering parameters and mass balance rather than from a directly measured XRF line [6].

RESULTS.

In the elemental report, the principal components were C* at 71.60 mass %, Fe at 16.30 mass %, S at 6.58 mass %, Si at 1.30 mass %, Cl at 1.22 mass %, and Ca at 1.18 mass %. The high iron content indicates the presence of iron-containing corrosion products originating from the pipe, orifice plate, or other metallic equipment. Silicon, calcium, aluminium, and magnesium may indicate mineral dust, sand, or process-derived solid particles.

The appreciable sulfur and chlorine contents indicate the presence of sulfur-containing and chlorine-containing constituents in the deposit. However, EDXRF does not determine the valence state of an element or identify a specific chemical compound. Consequently, sulfur cannot be assigned exclusively to SO_3, iron exclusively to Fe_2O_3, or chlorine to a specific chloride on the basis of the EDXRF result alone.

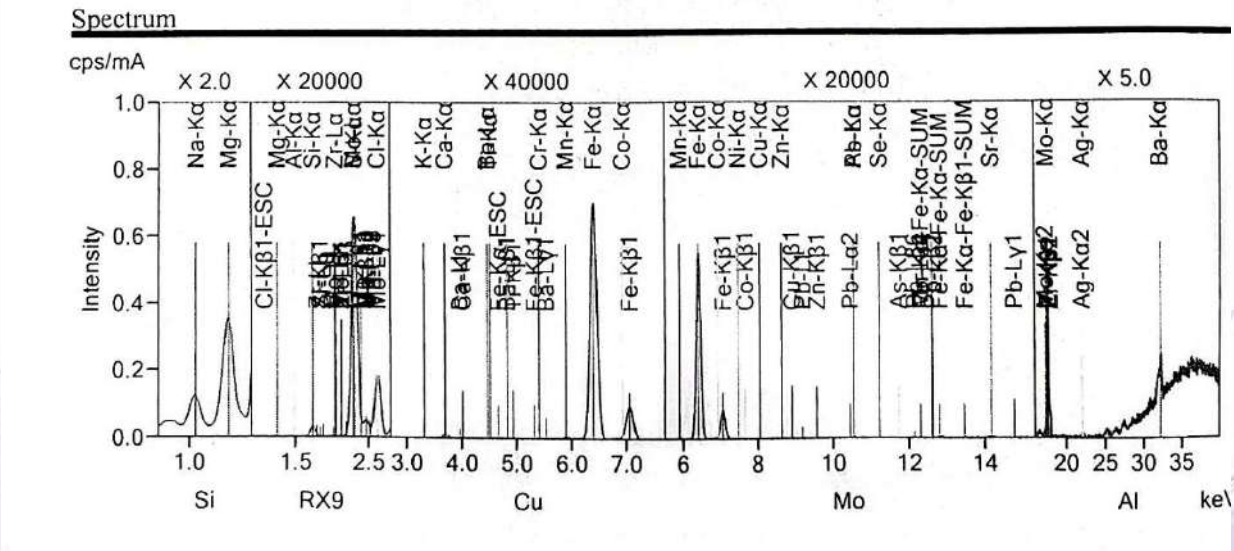


Figure 2. EDXRF spectrum of the perafor powder sample obtained with the NEX CG II instrument using the fundamental-parameters method.

ISSN 3030-3907

Table 3.

Elemental composition of the perafor sample (general FP calculation)

No.	Component	Result (mass %)	Stat. error	LLD	LLQ
1	C	71.60	—	—	—
2	Fe	16.30	0.0087	0.0003	0.0009
3	S	6.58	0.0032	0.0004	0.0012
4	Si	1.30	0.0030	0.0025	0.0074
5	Cl	1.22	0.0010	0.0003	0.0008
6	Ca	1.18	0.0040	0.0022	0.0067
7	Na	0.793	0.0527	0.0686	0.206
8	Zr	0.218	0.0009	0.0002	0.0005
9	Mg	0.205	0.0075	0.0078	0.0233
10	Al	0.196	0.0025	0.0054	0.0162
11	Mn	0.186	0.0009	0.0009	0.0026
12	K	0.0775	0.0019	0.0039	0.0116
13	Co	0.0274	0.0010	0.0029	0.0088
14	Sr	0.0206	<0.0001	<0.0001	0.0001
15	Cu	0.0198	0.0002	0.0002	0.0007
16	Ba	0.0180	0.0005	0.0011	0.0033
17	Ti	0.0097	0.0006	0.0015	0.0045
18	Eu	(0.0080)	0.0019	0.0058	0.0174
19	Hf	0.0079	0.0004	0.0011	0.0033
20	Ni	0.0065	0.0002	0.0003	0.0010
21	Cr	0.0062	0.0003	0.0007	0.0021
22	Zn	0.0052	0.0001	0.0001	0.0004
23	Br	0.0048	<0.0001	<0.0001	0.0002
24	As	0.0035	<0.0001	<0.0001	0.0002
25	Rb	0.0020	<0.0001	0.0002	0.0005
26	Te	0.0017	0.0001	0.0003	0.0009
27	Sn	0.0012	<0.0001	0.0002	0.0005

ISSN 3030-3907

No.	Component	Result (mass %)	Stat. error	LLD	LLQ
28	Nb	0.0009	<0.0001	0.0001	0.0004
29	Ag	0.0008	<0.0001	<0.0001	0.0002
30	Pb	(0.0007)	0.0001	0.0003	0.0010
31	Ga	(0.0003)	<0.0001	0.0001	0.0004

Note: LLD is the lower limit of detection and LLQ is the lower limit of reliable quantification. Values in parentheses are below the LLQ or were not confirmed by the algorithm as reliable quantitative results and should be interpreted only as indications of trace presence. The C value was estimated using the FP scattering/balance algorithm.

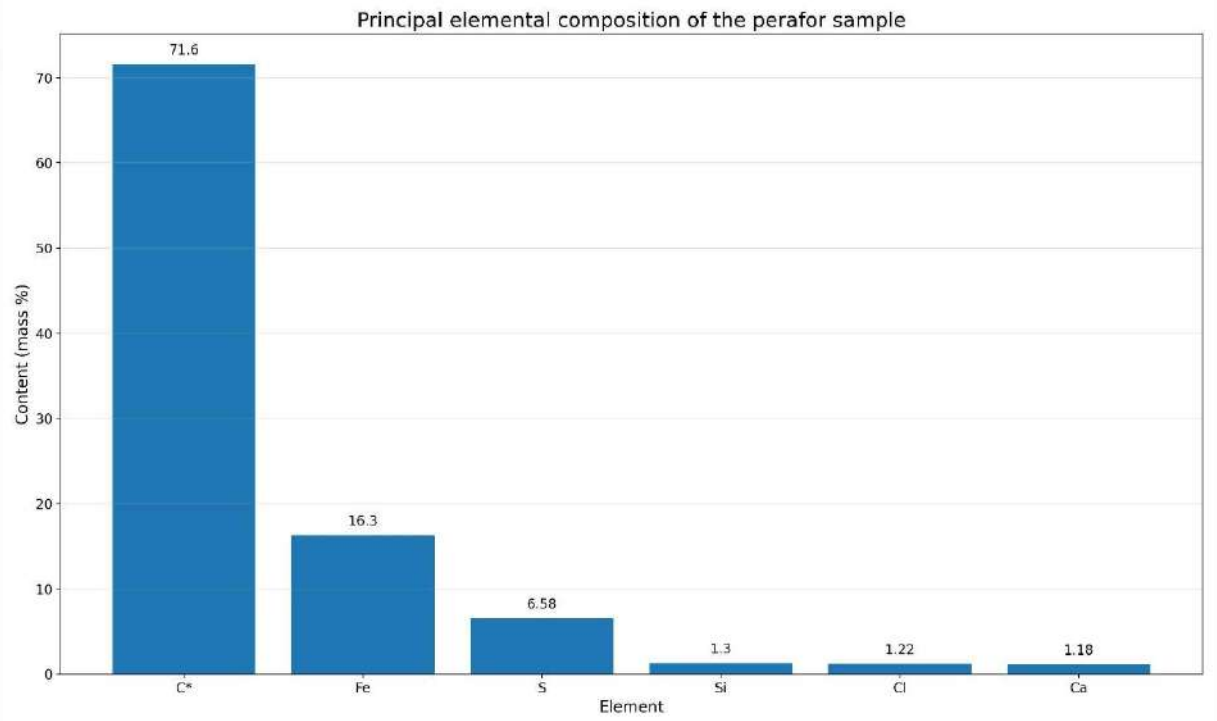


Figure 3. Distribution of the principal elements in the perafor sample (C* is the FP balance/matrix estimate).

Accordingly, the reported C = 71.60 mass % and C = 37.50 mass % values are not directly measured concentrations, but FP estimates obtained under two different normalization modes. Fe_2O_3, SO_3, SiO_2, and the other reported oxides are likewise not identified crystalline phases, but conditional oxide-equivalent representations of the corresponding elements [7].

ISSN 3030-3907

Table 4.

Oxide-equivalent composition of the perafor sample (FP calculation)

No.	Component	Result (mass %)	Stat. error	LLD	LLQ
1	C	37.50	—	—	—
2	Fe_2O_3	30.50	0.0143	0.0004	0.0013
3	SO_3	21.60	0.0070	0.0009	0.0028
4	SiO_2	3.63	0.0059	0.0049	0.0146
5	CaO	2.15	0.0073	0.0041	0.0124
6	Cl	1.61	0.0009	0.0003	0.0008
7	Na_2O	1.13	0.0645	0.110	0.329
8	Al_2O_3	0.489	0.0044	0.0093	0.0280
9	MgO	0.410	0.0113	0.0141	0.0422
10	ZrO_2	0.375	0.0022	0.0008	0.0023
11	MnO	0.324	0.0015	0.0014	0.0041
12	K_2O	0.119	0.0030	0.0062	0.0185
13	Co_2O_3	0.0460	0.0018	0.0055	0.0164
14	CuO	0.0345	0.0004	0.0003	0.0009
15	SrO	0.0319	0.0001	<0.0001	0.0002
16	BaO	0.0234	0.0009	0.0021	0.0064
17	TiO_2	0.0219	0.0012	0.0032	0.0097
18	NiO	0.0125	0.0003	0.0005	0.0014
19	Cr_2O_3	0.0117	0.0005	0.0013	0.0040
20	ZnO	0.0092	0.0002	0.0002	0.0006
21	As_2O_3	0.0071	0.0001	0.0001	0.0004
22	MoO_3	0.0024	0.0006	0.0007	0.0022
23	PbO	(0.0010)	0.0002	0.0005	0.0015
24	Ag_2O	0.0008	0.0001	0.0001	0.0004
25	SeO_2	(0.0002)	<0.0001	<0.0001	0.0003

The oxide-equivalent results represent software-calculated and normalized fractions obtained by converting the elements to conventional oxide formulae. The oxide-equivalent calculation reported C* at 37.50 mass %, Fe_2O_3 at 30.50 mass %,

ISSN 3030-3907

SO_3 at 21.60 mass %, SiO_2 at 3.63 mass %, CaO at 2.15 mass %, Cl at 1.61 mass %, and Na_2O at 1.13 mass %. The difference between the C* values in the elemental and oxide reports may be associated with the use of two different software matrix models and normalization schemes.

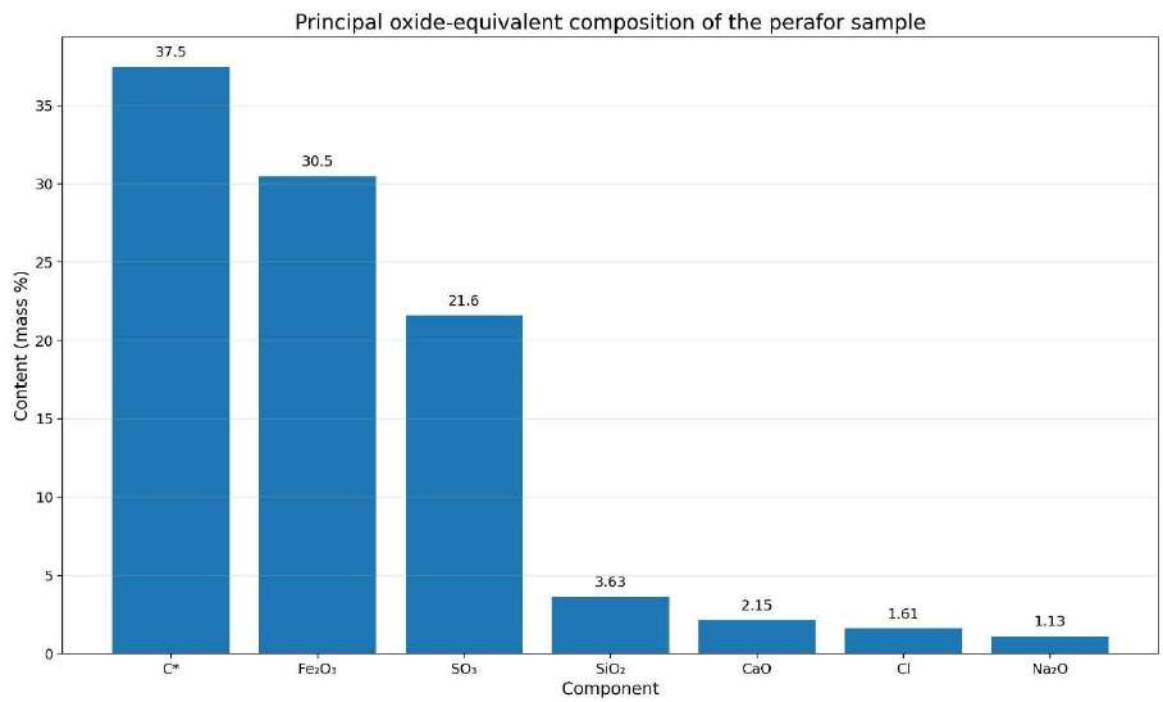


Figure 4. Distribution of the principal oxide-equivalent components in the perafor sample

Among the principal directly detected elements, Fe, S, Si, Cl, and Ca were present at 16.30, 6.58, 1.30, 1.22, and 1.18 mass %, respectively. The high iron content indicates that corrosion products detached from the orifice plate, pipeline, and other metallic components constitute a substantial fraction of the perafor. Si, Ca, Al, and Mg indicate the participation of sand, dust, and mineral particles. Chlorine indicates chlorine-containing constituents that, in an environment containing moisture or condensate, may increase the risk of localized and under-deposit corrosion. Sulfur at 6.58 mass % indicates the participation of sulfur-containing deposits or process contaminants, although their precise chemical form cannot be determined from XRF results alone [8-9].

In the oxide-equivalent mode, Fe_2O_3, SO_3, SiO_2, CaO, Cl, and Na_2O were reported at 30.50, 21.60, 3.63, 2.15, 1.61, and 1.13 mass %, respectively. Perafor should therefore not be considered solely as “soot” or “rust”, but as a mixed deposit comprising a carbonaceous binder, iron-containing corrosion products, sulfur-containing constituents, and mineral particles. Such a deposit can accumulate on the orifice bore and upstream edge, reduce the effective cross-sectional area, increase ΔP, and create a risk of overestimation of the gas flow rate.

DISCUSSION.

ISSN 3030-3907

To determine the forms of corrosion that may occur and identify potential solutions, a number of published investigations were analysed in relation to the composition of the gas transported through main gas pipelines.

Imidazoline is currently regarded as one of the most widely used and effective corrosion-inhibitor chemistries in industrial oil and gas applications. The efficiency of a volatile corrosion inhibitor synthesized on an imidazoline basis was evaluated for reducing top-of-the-line and bottom-of-the-line corrosion of carbon-steel pipelines in a CO_2-saturated environment. The authors tested an imidazoline produced from higher fatty acids and diethylenetriamine (DETA) under model conditions approximating those of a gas pipeline. Corrosion protection was analysed by weight-loss measurements, electrochemical impedance spectroscopy (EIS), potentiodynamic polarization (PDP), linear polarization resistance (LPR), scanning electron microscopy (SEM), energy-dispersive X-ray analysis (EDAX), and contact-angle measurements. At a concentration of 300 ppm, the inhibitor exhibited protection efficiencies of up to 91.6 % under bottom-of-the-line (BOL) conditions and 89.9 % under top-of-the-line (TOL) conditions. A decrease in the oxide layer and surface roughness, an increase in surface hydrophobicity, and adsorption consistent with the Langmuir isotherm were also reported. These observations indicate that imidazoline may be used as an effective volatile inhibitor in gas pipelines, particularly in regions containing condensate and a vapour phase. A major advantage of the study is that the inhibitor was shown to act not only in the liquid phase but also in the vapour–condensate TOL region, which represents a model close to actual operating conditions in main gas pipelines. A second advantage is the combined application of electrochemical, mass-loss, and surface-morphology methods, which provided mutually supporting results. Third, imidazoline was shown to function as a mixed-type inhibitor, simultaneously suppressing anodic and cathodic processes. The principal limitation is that only imidazoline itself was tested; a complex formulation containing a quaternary ammonium compound (QAC) and a dispersant was not evaluated. Furthermore, real pipeline contaminants such as under-deposit corrosion products, sand, rust, metal particles, or perafor were not modelled separately. Another limitation is that the results were obtained under laboratory conditions, and no long-term field-trial data were presented. Consequently, the study clearly demonstrates the baseline effectiveness of imidazoline, but further investigation is required before it can be regarded as a fully developed industrial solution for a complex mixed environment in a main gas pipeline [10].

The hydrolysis of an imidazoline corrosion inhibitor prepared from tall-oil fatty acid and diethylenetriamine (TOFA/DETA), and its effect on protection of X65 steel in a CO_2-saturated 3 wt.% NaCl medium, were investigated. The authors

ISSN 3030-3907

analysed the chemical evolution of the inhibitor with time, including hydrolysis of the imidazoline ring, protonation, and micelle formation. The results showed that, as hydrolysis proceeds, the composition and adsorption behaviour of the inhibitor change, directly affecting the efficiency of the protective film formed on the X65 steel surface. The hydrolysis process was accelerated in an acidic medium, imidazoline consumption followed pseudo-first-order kinetics, and the reported activation energy was 72.0 ± 2.9 kJ/mol. In addition, the "aged" inhibitor was found to affect general and localized corrosion differently. The work demonstrates that, when imidazoline-based inhibitors are applied to pipeline-grade X65 steel, not only their initial performance but also their time-dependent stability is of decisive importance. Rather than evaluating the inhibitor merely in terms of whether it works, the study provides an in-depth analysis of hydrolysis, protonation, micelle formation, and the adsorption mechanism, showing how compositional changes with time influence inhibition performance. A second important feature is the use of X65 steel as the test material, which makes the study highly relevant to main pipelines. The findings are practically significant for sweet-corrosion conditions, that is, a wet environment containing CO_2, and provide useful engineering information for selecting pipeline inhibitors. Nevertheless, the study was conducted in a laboratory CO_2-saturated brine and did not fully reproduce sand, rust, heavy-hydrocarbon deposits, turbulent flow, or a condensate-containing multiphase environment representative of an operating main gas pipeline. Only an imidazoline-based inhibitor was examined; complex formulations containing quaternary ammonium salts or a dispersant were not assessed. The article therefore mainly describes a laboratory mechanism rather than field-trial or long-term industrial operating results. Although the work explains the fundamental mechanism of imidazoline very well, additional practical testing is required before the formulation can be adopted directly as a ready industrial treatment [11].

In the study presented by Wong and Park, the effects of active corrosion-inhibitor components, particularly a quaternized amine monomer, on the growth of an iron-carbonate ($FeCO_3$) scale and on the development of protective properties at the metal surface under CO_2 conditions were investigated. The work showed that the $FeCO_3$ scale formed under sweet-corrosion conditions is not merely a corrosion product, but an important factor affecting inhibitor adsorption and film stability. The authors analysed how a quaternized-amine active component can enhance the protective mechanism at the metal surface in association with $FeCO_3$-scale formation. The study suggests that QAC or quaternized-amine components play an important role in increasing the density and stability of the protective film under sweet-corrosion conditions. It therefore provides a scientific basis for adding a quaternized amine to imidazoline-based inhibitor packages, particularly for main-

ISSN 3030-3907

pipeline corrosion in the presence of CO_2. The active component is analysed not only in terms of overall inhibition efficiency, but also through the mechanism associated with $FeCO_3$-scale formation, explaining the interaction of a QAC-type substance with the natural carbonate layer on the metal surface. This provides an important theoretical basis for the rational design of inhibitor packages for main gas pipelines. However, the study did not evaluate a complete complex formulation such as imidazoline + QAC + dispersant, but only the role of an individual active inhibitor component. A ready-to-use industrial formulation cannot therefore be derived directly from the work. In addition, factors characteristic of actual main-pipeline operation, including sand, rust, organic deposits, and under-deposit corrosion, were not specifically addressed. Although the article is a strong source for understanding the role of QACs, it should not be regarded as the sole evidence for the complete performance of a complex inhibitor package [12].

The study reported by Tsui and co-authors examined the effects of active corrosion-inhibitor components on the formation of an iron-carbonate ($FeCO_3$) layer on carbon steel in a CO_2 environment. The principal emphasis was placed on the interaction of quaternized-amine active substances with the $FeCO_3$ scale and the mechanism by which this interaction improves the effectiveness of the protective film. The authors showed that, under sweet-corrosion conditions, the iron-carbonate layer may act as a natural protective film on the internal pipeline surface, while quaternized-amine components influence the kinetics and compactness of layer formation and thereby enhance its corrosion-protection properties. According to the findings, some active inhibitor components may retard $FeCO_3$-scale formation, whereas quaternized-amine components can support its formation and promote a denser and more stable protective layer on the metal surface. The work therefore provides a scientific explanation for the use of QAC components in complex inhibitor packages for sweet-corrosion environments. Although the article is highly informative for understanding the role of QACs, it does not by itself demonstrate the complete performance of a complex formulation [13].

A subsequent investigation evaluated the performance of quaternary-amine corrosion inhibitors as a function of hydrocarbon-chain length and temperature. The authors synthesized C10-, C12-, and C16-chain quaternary-amine inhibitors and examined their protective properties for coiled-tubing steel in concentrated HCl by gravimetric and electrochemical methods. At low temperature, inhibitors with longer hydrocarbon chains showed higher efficiency: at 30 °C and 50 ppm, the protection efficiencies of the C16, C12, and C10 inhibitors were 80.4 %, 78.3 %, and 67.2 %, respectively. However, when the temperature was increased to 90 °C, this order changed and the overall efficiency decreased. The study demonstrates

ISSN 3030-3907

that the anticorrosion action of quaternary-amine inhibitors depends not only on the functional groups, but also directly on hydrocarbon-chain length, solubility, and temperature. It is therefore an important source for understanding structure–performance relationships when selecting a QAC type. However, the investigation was not performed under sweet-corrosion conditions in a main gas pipeline, but in concentrated HCl, which is closer to an acidizing environment. Direct transfer of the conclusions to a gas-pipeline environment containing CO_2, moisture, and condensate therefore requires caution. Another limitation is that only QAC-type inhibitors were considered, without evaluation of a complex formulation containing imidazoline or a dispersant [14].

In their review, Wang, Pang, and Zheng comprehensively analysed under-deposit corrosion (UDC) in oil and gas pipelines. They identified UDC as a serious threat to safe pipeline operation and systematically summarized test methods, corrosion mechanisms, and mitigation strategies. Two deposit-modelling methods and three UDC test systems were reviewed, and two principal UDC mechanisms were discussed in relation to the degree of deposit coverage and its protective characteristics. Uneven deposit distribution, which creates a galvanic couple, was identified as a principal cause of localized corrosion. Scale control and corrosion inhibition were considered important approaches for reducing UDC, and the need to develop more representative deposit models, effective UDC inhibitors, and in-situ monitoring technologies was emphasized. This article is an important theoretical and practical source for understanding deposits, perafor, and localized-corrosion phenomena. It provides strong support for explaining under-deposit corrosion mechanisms and the potential need for dispersant-assisted control, although additional specialized experimental studies are required to develop a specific formulation [15].

Fayyad and co-authors published a study in 2024 that used a laboratory approach close to practical conditions to evaluate under-deposit corrosion of carbon steel. The study was performed in a CO_2/sulfide environment using a sulfate-containing CO_2-saturated brine at 60 °C and a reported test concentration of 1000 ppm. The effects of different mineral deposits, namely FeS_2, FeS, and SiO_2 (sand), on inhibitor efficiency were examined. The authors separately evaluated deposit type, particle characteristics, and complete or partial coverage of the steel surface. According to EIS, morphology, and elemental-analysis results, a commercial UDC inhibitor showed its highest performance at 400 ppm. After 6 h, reported inhibition efficiencies were 77.5 % for FeS, 94.5 % for FeS_2, and 94.6 % for SiO_2. At the same time, the authors showed that the inhibitor did not reach the steel surface beneath all deposits to the same extent: it performed effectively in the presence of FeS and SiO_2, whereas access to the steel surface beneath the FeS_2

ISSN 3030-3907

deposit was limited. EDX and XPS analyses confirmed that the inhibitor could penetrate some deposits and adsorb on the metal surface. Although this study is close to the problem considered here, it did not fully reproduce multiphase flow, pressure variation, heavy-hydrocarbon condensate, or long-term operation in an actual main gas pipeline. Nevertheless, its demonstration that deposits, rust, sand, and corrosion products can accumulate in metering assemblies and main pipelines provides scientific support for investigating the addition of a dispersant [16].

Yang and co-authors reported in 2024 on the synergistic effect of thioureido imidazoline (TU-IM) and cationic surfactants with different carbon-chain lengths in reducing corrosion of X80 steel in a CO_2-saturated NaCl solution. TU-IM was evaluated both separately and together with cationic additives, including dodecyltrimethylammonium bromide (DTAB) and tetradecyltrimethylammonium bromide (TTAB). When TU-IM and the cationic surfactants were used together, the inhibition efficiency increased sharply. The best result was obtained with a combination of 10 mg/L TU-IM and 10 mg/L DTAB/TTAB, for which the corrosion-inhibition efficiency reached 97.68 %. The authors attributed this behaviour to cooperative adsorption of the two components on the metal surface, formation of a denser and more stable protective film, and intermolecular interactions. The article shows that the corrosion-protection effect of an imidazoline derivative can be enhanced by introducing an additional cationic component, thereby providing scientific support for the use of QAC or QAC-like cationic additives in complex inhibitor packages. The work investigated synergy with QAC-like cationic surfactants rather than a conventional oilfield QAC package, and no dispersant was added. It therefore demonstrates primarily adsorption-protection synergy rather than dispersion of deposits or reduction of perafor. The principal concept that can be derived from the study is that addition of a cationic component to an imidazoline-based formulation can increase film stability. The protection efficiency increased substantially when the imidazoline derivative was used together with the cationic additive. This source can therefore provide an important scientific basis for including QAC or QAC-like additives in a complex inhibitor formulation [17].

Patent CN104233310B describes a complex corrosion inhibitor based on an imidazoline quaternary ammonium salt and a method for its preparation. The disclosed composition contains functional components such as an alkyl-acid imidazoline quaternary ammonium salt, a dispersant, a co-solvent, a surfactant, and a phosphonate. The technology first forms an imidazoline from a fatty acid and a polyamine, after which the product is quaternized with benzyl chloride and then combined with the dispersant and other auxiliary components. According to the patent, the imidazoline-formation stage is conducted at approximately 140–180 °C,

ISSN 3030-3907

followed by formation of the quaternary ammonium salt. This source provides a technological basis for the structure, function, and preparation sequence of a complex formulation. However, additional laboratory and pilot testing would be required before the patented composition could be regarded as a proven, ready industrial solution directly suitable for a purified-gas environment in a main gas pipeline [18].

CONCLUSIONS.

In this study, a black powder (perafor) sample collected from the orifice-metering assembly of a gas distribution station was characterized by energy-dispersive X-ray fluorescence spectrometry (EDXRF). The principal directly detected elements were Fe at 16.30 mass %, S at 6.58 mass %, Si at 1.30 mass %, Cl at 1.22 mass %, and Ca at 1.18 mass %. The results demonstrated that perafor should be regarded not merely as soot or rust, but as a complex heterogeneous deposit consisting of iron-containing corrosion products, sulfur-containing components, and mineral particles.

Determination of the perafor composition indicates that it is advisable to reduce processes such as agglomeration of perafor particles, adhesion caused by condensate and heavy hydrocarbons, attachment to the orifice-plate and pipeline surfaces, and formation of a dense layer in filters by means of a dispersant [19–22].

When purified natural gas is transmitted into a main gas pipeline, adding a dispersant formulation not as a general additive to the entire gas stream, but at sections where moisture and condensate occur, at low points, in post-compressor cooling zones, upstream of GDS filters and metering assemblies, and in lines where perafor regularly accumulates may provide a solution to the problems described above.

REFERENCES

1. Akhmedova, O. B.; Akhmedova, Sh. U. Creation of effective absorbent composition for absorption gas purification. Universum: Technical Sciences 2024, 11(128). https://doi.org/10.32743/UniTech.2024.128.11
2. Atamov, A. A. Protection of main pipelines against corrosion. Ikro Journal 2025, 15(01), 754–758. [In Uzbek].
3. Axmedova, O. B.; Boltayev, S. S. Effect of a local demulsifier on oil desalination and dehydration; use of a low-temperature separator in gas preparation. In Proceedings of the V International Conference-Symposium on Chemical Technology and Nanotechnology Research in High-Molecular Compounds, Organic Substances and Composite Materials: Problems and Solutions, Tashkent, Uzbekistan, November 2021.

ISSN 3030-3907

4. Tamalmani, K.; Husin, H. Review on corrosion inhibitors for oil and gas corrosion issues. Applied Sciences 2020, 10, 3389. https://www.mdpi.com/2076-3417/10/10/3389

5. International Organization for Standardization. ISO 5167-2:2022. Measurement of fluid flow by means of pressure differential devices inserted in circular cross-section conduits running full—Part 2: Orifice plates, 2nd ed.; ISO: Geneva, Switzerland, 2022.

6. Beckhoff, B.; Kanngießer, B.; Langhoff, N.; Wedell, R.; Wolff, H., Eds. Handbook of Practical X-Ray Fluorescence Analysis; Springer: Berlin/Heidelberg, Germany, 2006. https://doi.org/10.1007/978-3-540-36722-2

7. Colahan, M.; Young, D.; Singer, M.; Nogueira, R. P. Black powder formation by dewing and hygroscopic corrosion processes. Journal of Natural Gas Science and Engineering 2018, 56, 358–367. https://doi.org/10.1016/j.jngse.2018.06.021

8. He, J.; Wang, D.; Guo, D.; Xie, F.; Qin, Y. Generation causes of black powder in the east line of the gas supply pipeline from the Liaohe oilfield: Analysis and discussion. Engineering Failure Analysis 2022, 139, 106506. https://doi.org/10.1016/j.engfailanal.2022.106506

9. Reader-Harris, M. J.; Barton, N.; Hodges, D. The effect of contaminated orifice plates on the discharge coefficient. Flow Measurement and Instrumentation 2012, 25, 2–7. https://doi.org/10.1016/j.flowmeasinst.2011.11.003

10. Yotapan, N.; Sriplai, N.; Ruengsangtongkul, S.; Sombatmankhong, K. Imidazoline as a volatile corrosion inhibitor for mitigation of top- and bottom-of-the-line CO_2 corrosion in carbon steel pipelines. Langmuir 2024, 40(23), 11888–11902. https://doi.org/10.1021/acs.langmuir.3c03827

11. Shamsa, A.; Barmatov, E.; Hughes, T. L.; Hua, Y.; Neville, A.; Barker, R. Hydrolysis of imidazoline-based corrosion inhibitor and effects on inhibition performance of X65 steel in CO_2-saturated brine. Journal of Petroleum Science and Engineering 2022, 208, 109235. https://doi.org/10.1016/j.petrol.2021.109235

12. Wong, J. E.; Park, N. G. Effect of corrosion-inhibitor active components on the growth of iron-carbonate scale under CO_2 conditions. In CORROSION 2008, New Orleans, LA, USA, 16–20 March 2008; AMPP/NACE.

13. Tsui, K.; Wong, J. E.; Park, N. G. Effect of corrosion-inhibitor active components on the formation of iron carbonate on carbon steel. In CORROSION 2010; NACE International, 2010.

14. Al-Taq Ali, A. A.; Ali Shaikh, A.; Alrustum Abdullah, A. Performance variation of quaternary-amine corrosion inhibitors as a function of hydrocarbon-chain length with respect to temperature. In SPE International Oilfield Corrosion Conference and Exhibition, Aberdeen, Scotland, 18–19 June 2018. https://doi.org/10.2118/190900-MS

15. Wang, Z. B.; Pang, L.; Zheng, Y. G. A review on under-deposit corrosion of pipelines in oil and gas fields: Testing methods, corrosion mechanisms and mitigation strategies. Corrosion Communications 2022, 7, 70–81. https://doi.org/10.1016/j.corcom.2022.03.007
16. Fayyad, E. M.; Sliem, M. H.; Al-Qahtani, N.; Ryan, M. P.; Abdullah, A. M. Assessing under-deposit corrosion inhibitor performance for carbon steel in a CO_2/sulfide environment. Journal of Materials Research and Technology 2024, 28, 1433–1451. https://doi.org/10.1016/j.jmrt.2023.11.244
17. Yang, G.; Qi, H.; Wu, X.; Liu, A.; Zhang, S.; Zhang, J. Synergistic inhibition effect of thioureido imidazoline and cationic surfactants with different alkyl-chain lengths on X80 carbon steel in CO_2-saturated NaCl solutions. International Journal of Electrochemical Science 2024, 12, 100869. https://doi.org/10.1016/j.ijoes.2024.100869
18. Guo, K.; Zhou, P. Compound imidazoline quaternary-ammonium-salt corrosion inhibitor and preparation method thereof. Chinese Patent CN104233310B, 2016. https://patents.google.com/patent/CN104233310B/en
19. Akhmedova, O. B.; Nurullaeva, Z. V.; Komilov, M. Z.; Asadova, D. F.; Razhabov, R. N.; Fozilov, S. F. Basic directions of application of low-molecular polyethylene from local secondary raw materials. Universum: Technical Sciences 2019, 11(68). https://doi.org/10.32743/UniTech.2019.68.11-3
20. Fozilov, S. F.; Akhmedova, O. B.; Mavlonov, Sh. B.; Saidakhmedov, Sh. M.; Khamidov, B. N. Synthesis and investigation of the properties of depressant additives based on heterocyclic esters of polymethacrylic acids. Uzbek Journal of Oil and Gas 2010, 4, 41–42. [In Russian].
21. Akhmedova, O.; Hojiyeva, R.; Hayitov, R.; Qayumov, A.; Maxmudov, N.; Asadova, R.; Murtazaev, A.; Narimov, R.; Khikmatova, D.; Abdalimov, A. Production of low-sulfur fuel distillates from waste tyres via pyrolysis and their application in petroleum refining. Journal of Ecological Engineering 2026, 27(8), 106–122. https://doi.org/10.12911/22998993/220257
22. Turabdjanov, S. M.; Fozilov, H. S.; Axmedova, O. B.; Fozilov, S. F. Mathematical modelling and optimisation of the reactor for the esterification of safflower oil with n-butyl alcohol. Technical Science and Innovation 2026, 1, 37–41, Article 9. https://doi.org/10.59048/2181-1180.1817